Reversal Processes in FePt Nanoparticle Arrays

Dieter SUESS, Thomas SCHREFL, Josef FIDLER, Robert C. WOODWARD, Timothy G. ST. PIERRE, Robert STREET, Shouheng SUN, Christopher MURRAY, Liesl FOLKS and Bruce TERRIS

***Abstract*-- Magnetic measurements were made on arrays of chemically synthesized FePt nanoparticles. The results show J_r/J_s ratios of 0.6 which is greater than that predicted for a series of non-interacting Stoner-Wohlfarth particles. The samples also displayed a high component of reversible magnetization and open recoil loops, all of which are reminiscent of exchange coupling between particles or grains. However, the particles in the arrays are well separated and so micromagnetic modeling was preformed in order to understand the source of these interactions. It was found that the experimental behavior could only be replicated within the micromagnetic model when inhomogeneous magnetization occurred within the FePt Nanoparticles. This occurred only when there were both multiple c-axes within the FePt nanoparticles and a reduction of the exchange stiffness (A) compared to literature values of bulk FePt.**

***Index Terms*-- FePt, nanoparticles, micromagnetic modeling, Stoner-Wohlfarth model, remanence enhancement, exchange stiffness.**

I. Introduction

Small magnetic particles are the basic structural units of magnetic recording media. To achieve a high storage density and obtain a high thermal stability a small particle size and high magneto-crystalline anisotropy are required. Recently, Sun and coworkers [1,2] fabricated monodisperse FePt nanoparticles. The particles were chemically synthesized with various compositions and sizes. The particles self-assemble into a three-dimensional superlattice when deposited onto a suitably prepared substrate. The particles can be made with sizes varying from 3 to 10 nm with very narrow size range distributions. The magneto-crystalline anisotropy of the particles after annealing was found to be of the order of 10^6 J/m^3. The large anisotropy, the small particle size, and the high packing fraction makes self assembled FePt superlattices an ideal candidate for future high-density storage media with an areal density in the Tb/in^2 regime.

This work compares magnetic measurements and finite element micromagnetic simulations of magnetization processes of a three dimensional matrix of FePt nanoparticles.

II. Experimental Measurements

Samples of monodisperse FePt nanoparticles were prepared in accordance with the method outlined in [1,2]. The composition of the FePt nanoparticles was $Fe_{56}Pt_{44}$, with a particle diameter of 4nm. A solution containing the monodisperse FePt nanoparticles was allowed to evaporate and the subsequent powder heat-treated at 560°C for 30 minutes.

Magnetic measurements were made on pressed cylinders of the powders using an Aerosonics Vibrating Sample Magnetometer and either a 5T or a 12T Oxford Instruments superconducting solenoid. A hysteresis loop, recoil curve and recoil loop for this material are shown in Figure 1.

The value of J_s for the FePt nanoparticles was 1.31 T. The literature value for bulk FePt is approximately 1.44 T [3]. The J_r/J_s ratio (J_s measured in a 12T field) is 0.6 and the coercivity is around 0.6 MA/m. The recoil curve shows a high reversible component whilst the recoil loop is open. These effects and the high J_r/J_s ratio are often associated with the presence of exchange coupling between particles or grains [3]. However,

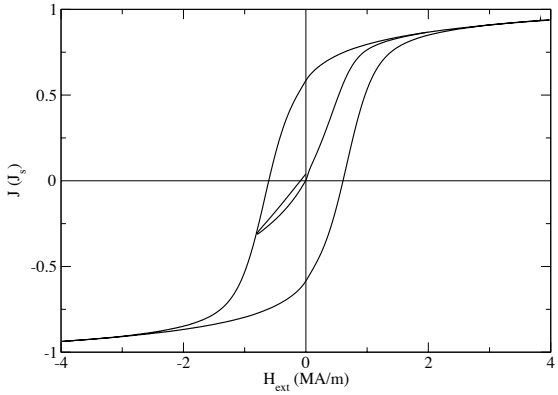

Fig. 1. Hysteresis loop, recoil curve and recoil loop for FePt nanoparticle array.

Manuscript received November 19, 2001. This work was supported by the Austrian Science Fund (P13260 and Y132-PHY) and the Australian Research Council (ARC Large Grant 6994108)

D. Suess, T. Schrefl, and J. Fidler are with the Institute of Applied and Technical Physics, Vienna University of Technology, Wiedner Hauptstr. 8–10, A-1040 Vienna, Austria (telephone: +43-1-5 8801-13729, fax: +43-1-58801-13798, dieter.suess@tuwien.ac.at).

R. C. Woodward, T. G. St. Pierre, R. Street are with the Department of Physics, The University of Western Australia, 35 Stirling Hwy, Crawley 6009, Australia (woodward@physics.uwa.edu.au)

S. Sun, C. Murray are with the IBM Watson Research Center, Yorktown Heights, NY 10598, USA

L. Folks and B. Terris are with the IBM Almaden Research Center, 650 Harry Road, San Jose, CA, 95210, USA

the TEM work of Sun et al [1] suggests that the nanoparticles are well separated by the carbon matrix. It seem unlikely that there would be exchange coupling across the carbonaceous material, which separates the nanoparticles at room temperature and so the source of these exchange interactions is unknown.

In order to elucidate the source of the magnetic behavior of these nanoparticulate arrays we have preformed a series of micromagnetic simulations.

III. MODEL

To simulate the hysteresis loop and the reversal process for FePt nanoparticles particles we have applied a micromagnetic approach. The hysteresis loops are obtained by solving the Landau-Lifshitz-Gilbert equation for different external fields around the loop. For each field the LLG equation is integrated using a BDF formulae [5]. When equilibrium is reached, the field is stepped to the next value of the external field. We define our system to be in equilibrium if the change of the normalized magnetization divided by the time step, $|d\mathbf{u}/dt|$, becomes smaller than 10^{-4} on every node. In order to solve the boundary value problem for the scalar potential u we use a hybrid finite element/boundary element method proposed by Fredkin and Koehler [6]. The demagnetizing field is then given by the negative gradient of the scalar potential u, which is interpolated using linear shape functions.

A. Single c-axis

Figure 2 shows the arrangement of the FePt nanoparticles we have used for our simulations. The particles form a cubic array. The diameter of the particles is 4nm and the space between nearest neighbors is 2nm. The intrinsic properties of the FePt spheres are $A = 10.8 \times 10^{-12}$ J/m [7], $J_s = 1.31$ T and $K_1 = 5.9 \times 10^6$ J/m^3 [1]. One uniaxial easy axis is assigned to each FePt particle. The direction of the easy axis is randomly oriented over all the particles. The average mesh size is about 0.5nm, which leads to about 65000 finite elements for the whole model.

The configuration shown in Figure 2 (a) and (b) are the stable states for remanence ($H_{ext} = 0$) and for a point just passed coercivity ($H_{ext} = 4.8$ MA/m), respectively. The normalized z-component of the magnetic polarization is color-coded.

Figure 3 shows the hysteresis loop and a recoil curve for this FePt-array. The calculated hysteresis loop is very similar to that of an ensemble of non-interacting uniaxial particles with random orientation of the easy axes. In agreement to the predictions of the model of non-interacting single domain particles the hysteresis loop in Figure 3 has a remanence of $J_r/J_s = 0.5$ and a coercivity of 0.48 H_A [8].

In order to prove that the stray field interactions between the FePt particles are negligible we have performed two sets of hysteresis loop calculations, with and without the calculation of stray field interaction. The hysteresis loops are almost the same and the coercive fields differ by less than 0.05%. It appears therefore that the stray field interaction between the FePt particles does not significantly influences the switching

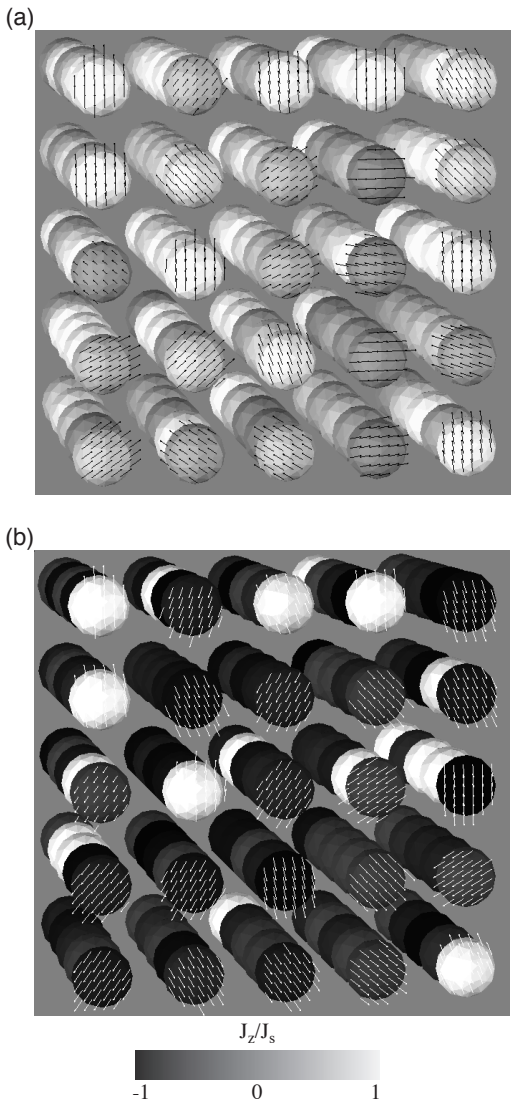

Fig. 2. Micromagnetic modeling of the transient states during reversal. Every FePt particle has one easy axis, randomly orientated. The images (a) and (b) correspond to states marked in Fig. 3.

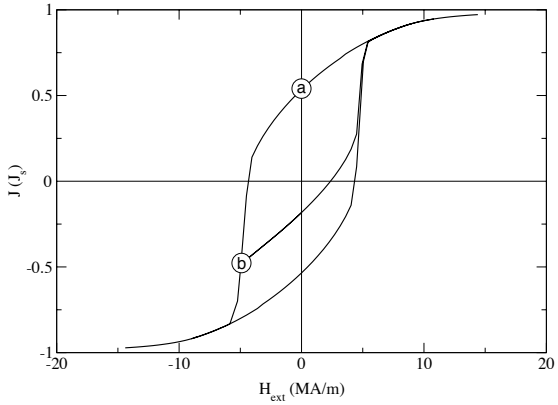

Fig. 3. Hysteresis loop and recoil curve obtained from micromagnetic modeling of an array of FePt particles with a single easy axis orientated at random.

process.

If the results according to this simple model are compared with the earlier experiments significant differences can be found.

- The coercive field of the computer simulations (4.3 MA/m) is about 8 times larger than the experimentally measured values (0.6 MA/m).
- The model does not lead to the measured remanence enhancement of $J_r/J_s = 0.6$
- The slope of the recoil curve in Figure 3 is much smaller than those observed in the experiment (figure 1)

B. Multiple c-axis

In order to obtain a better agreement with the experimental results we have assumed that the nanoparticles may consist of three independent c-axes oriented at 90° to each other. Such a distribution of the c-axis has been observed in a slightly different system by Bian et al. [9]. HREM images show an ordered $L1_0$ FePt nanoparticle, with a diameter of ~ 6-8nm, in a α–Al_2O_3 matrix with three different c-axes within the nanoparticle. Other complex FePt nanoparticles have also been observed by Watanabe et al. [10]. The multiple c-axes within a single nanoparticle are orthogonal to each other because of the transformation between the face centered cubic A1 phase and the tetragonal $L1_0$ phase. Where the c-axis in the $L1_0$ phase is along one of the <100> directions in the face centered cubic structure [11]. Other complex states within a nanoparticle including surface anisotropies are possible but may be better modeled using alternative techniques.

To consider multiple c-axes within each nanoparticle we subdivide every sphere into 8 octants ($o_{k,i}$). For every sphere (k), three orthogonal directions (a_k, b_k, c_k) are calculated, however the orientation of this triple is chosen at random. To every octant $o_{k,i}$ one of the axis a_k, b_k or c_k is assigned randomly. Figure 4 shows the distribution of the c-axes for one FePt particle. The different colors show different directions of the c-axes within each octant.

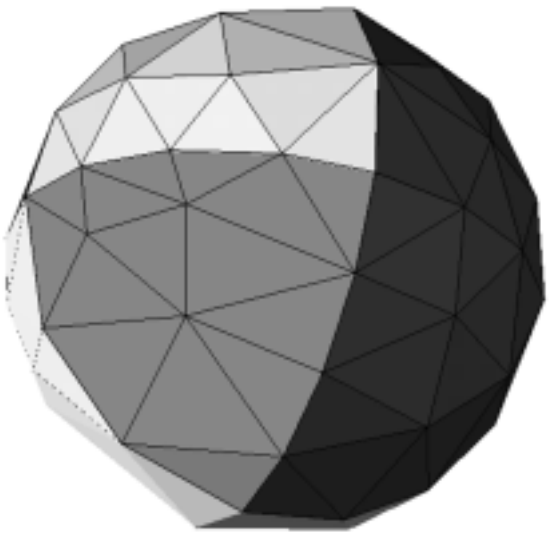

Fig. 4. One possible distribution of the c-axes within one FePt particle. The different colors correspond to regions with different c-axes orientations.

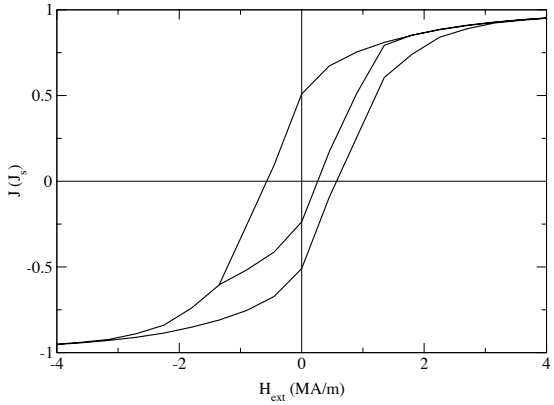

Fig. 5. Hysteresis loop and recoil curve obtained from micromagnetic modeling of an array of FePt particles with multiple c-axes within each particle.

The hysteresis loop and recoil loop for a set of particles with multiple c-axes is given in figure 5. The coercive field decreases by a factor 9 compared to the sample with only one easy axis within each particle. The relative slope of the initial part of the recoil loop is marginally higher than the single c axis model, shown in Figure 3, but still well below that observed experimentally. The magnetization reverses coherently at all stages of the reversal process so that the distribution of magnetization in the model looks exactly the same as seen in Figure 2 for the case of a single c axis per particle. There is no remanence enhancement using an exchange stiffness, $A = 10.8\ 10^{-12}$ J/m, and the FePt superlattice behaves like a Stoner-Wohlfarth system, but with a reduced effective anisotropy.

If the magnetization within each particle remains homogenous all the time, the anisotropy energy for one particle can be expressed as,

$$E_{tot} = E_0 - K_1 \sum_{i=1}^{3} (\mathbf{u}_i \mathbf{k}_i)^2 V_i \quad , \tag{1}$$

where $\mathbf{u_i}$ and $\mathbf{k_i}$ are the unit vectors of the magnetization and the easy axis in the region i, respectively. If the directions of k are orthogonal in the three regions within one particle (e.g. k_1=(1,0,0), k_2=(0,1,0) and k_3=(0,0,1)), equation 1 becomes

$$E_{tot} = E_0 - K_1 (V_1 u_x^2 + V_2 u_y^2 + V_3 u_z^2) \quad . \tag{2}$$

Figure 6 shows energy density surfaces. For every direction of the magnetization ***m***, the corresponding crystalline energy density is the distance from the origin to the point of the surface lying along the direction ***m***. Figure 6a shows the energy surface for the case that the fractions of V1, V2 and V3 to the total volume are 5%, 20% and 70%, respectively. For comparison, Figure 6b shows the energy surface for a cubic anisotropy. Note if the three volumes are the same, no anisotropy occurs.

Even with the reduced effective anisotropy, which produces a coercivity of the same order as seen in the experimental system, the effect of the stray field interactions is small. The stray field interactions have little or no effect over loop shape and do not result in remanence enhancement. The variation of

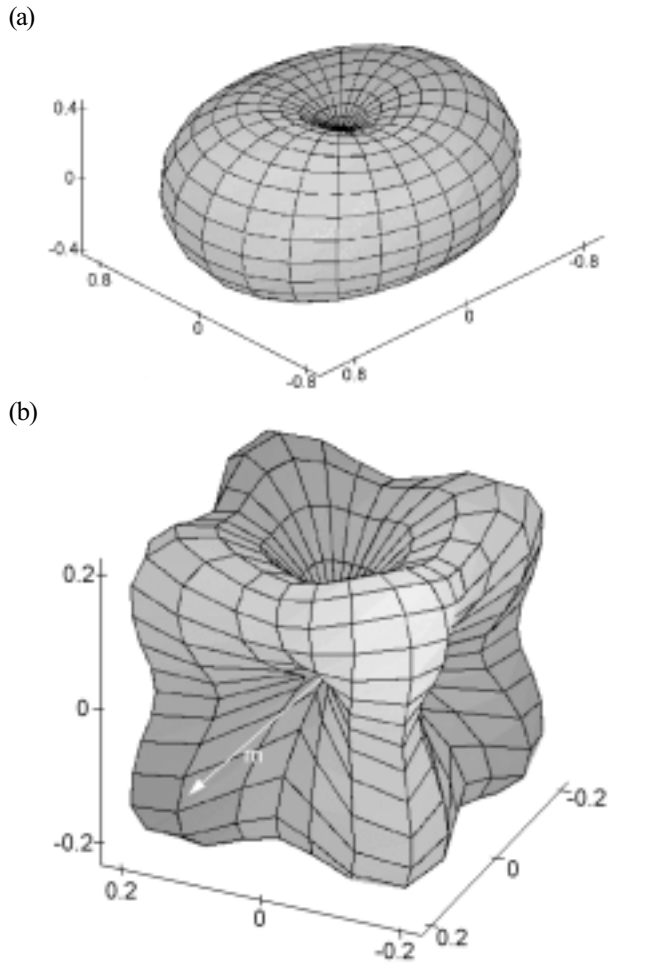

Fig. 6. Energy density plots of the crystalline anisotropy in arbitrary units. The upper image (a) shows the crystalline anisotropy energy density for the case that three orthogonal c-axes occur within one grain. The picture below (b) shows the energy density for cubic anisotropy.

the coercivity with and without stray fields is less than 1 %.

C. Reduction in exchange stiffness

In order to produce remanence enhancement in the multiple c-axes nanoparticles we investigated the effect of changes in the exchange stiffness (A). With smaller exchange stiffness the coercive field increases (Table 1) due to the formation of inhomogeneous states within one particle and remanence enhancement can be observed. It has been suggested that a reduction in the exchange interactions in ultra fine particles can be caused by the lower coordination of near surface atoms [12].

For zero exchange, there would be no coupling between the regions with different easy axes. The coercive field would increase to that of non-interacting Stoner-Wohlfarth particles.

In the case of strong coupling, the magnetization within one nanoparticle remains homogeneous looking similar to Figure 2 but with a reduced effective anisotropy. The effective anisotropy of the particle, as mentioned above, is related to the volume fractions of the three orthogonal components, V_1, V_2 and V_3, and can be calculated according to equation 1. The effective anisotropy (Figure 5a) is uniaxial but smaller in magnitude than the anisotropy of a particle with only one c-axis direction. An array of FePt particle with multiple c-axes and a strong exchange coupling then behave like an ensemble of non-interacting Stoner-Wohlfarth particles with a reduced anisotropy. As a consequence $J_r/J_s = 0.5$, and there is no observable remanence enhancement.

TABLE I
COERCIVE FIELD AND REMANENCE OBTAINED FROM MICROMAGNETIC MODELING OF AN ARRAY OF FEPT PARTICLES WITH MULTIPLE C-AXES FOR DIFFERENT VALUES OF EXCHANGE STIFFNSS (A).

A (J/m)	*H_c (kA/m)*	*J_z/J_s*
0. 10 x 10^{-11}	*1441*	*0. 62*
0. 36 x 10^{-11}	*901*	*0. 58*
1. 08 x 10^{-11}	*540*	*0. 51*

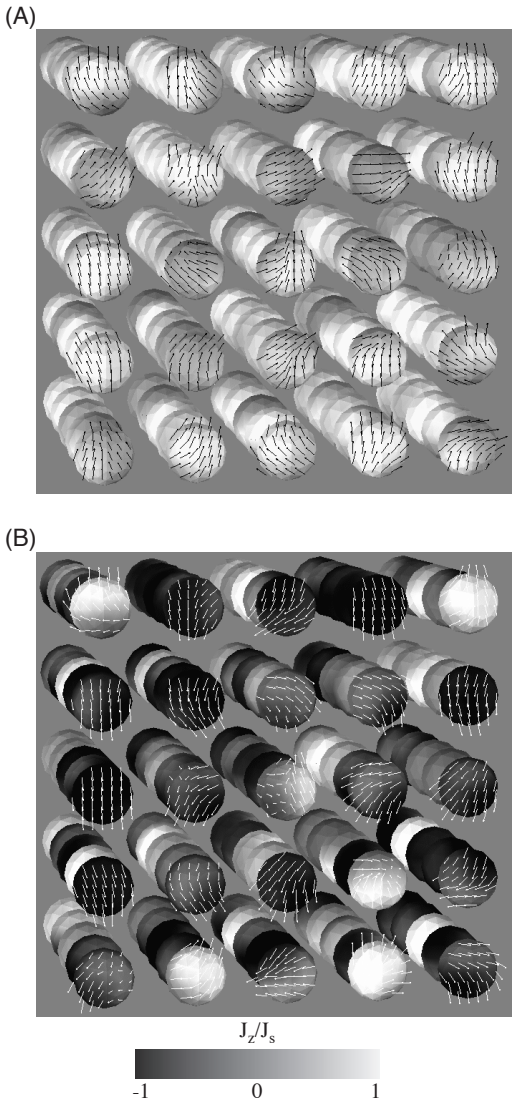

Fig. 7. Micromagnetic modeling of the transient states during reversal. Every FePt particle has multiple orthogonal c-axes, randomly orientated. The images (A) and (B) correspond to applied fields and magnetization marked in Fig. 8.

Remanence enhancement is only observed when the magnetization becomes inhomogeneous within one spherical FePt particle. This is observed when the exchange stiffness is reduced as shown in Figure 7, where the exchange stiffness has been reduced to A = 0.1 x 10^{-11} J/m. At zero external field the magnetization tend to point parallel to the different easy axes within one nanoparticle, but the exchange coupling between regions with different easy axes results in deviations of the magnetization from the easy direction and the production of remanence enhancement. As well as displaying remanence enhancement the multiple c axis model with reduced exchange stiffness also shows steeper recoil curves (Figure 8) which are similar to those seen in the experimental system.

Again, reference calculations without any magnetostatic simulations leads to only small variations in the coercivity with the general shape of the hysteresis loop and recoil curve are essentially unchanged. Thus, it can be concluded that the remanence enhancement and steep recoil behavior observed in the simulations as well as in the experiments are solely due to inhomogeneous magnetization processes within the FePt nanoparticles.

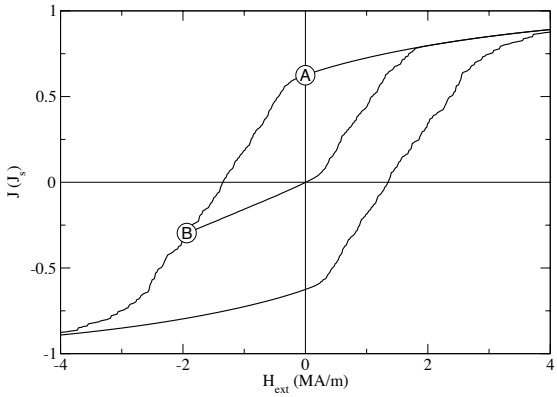

Fig. 8. Hysteresis loops and recoil curve obtained from micromagnetic modeling of an array of FePt particles with multiple c-axes within each particle exchange stiffness A = 0.1 x 10^{-11} J/m.

IV. Conclusions

Experimental observations of FePt nanoparticles arrays show remanence enhancement and reversible magnetization behavior reminiscent of materials with significant exchange coupling between magnetic grains. The modeling results presented here show that magnetostatic interactions have very little effect on the magnetization behavior of the nanoparticle arrays. Remanence enhancement and reversible magnetization behavior was produced within the models only when the magnetization within the FePt nanoparticles was inhomogeneous. To achieve inhomogeneous reversal of the magnetization within the FePt nanonparticles required both multiple c-axes within a nanoparticle and reduced exchange stiffness in comparison to literature values for FePt bulk alloys. The coercivity calculated for these particles, which reverse inhomogenously, was similar to that observed experimentally.

Acknowledgment

The authors wish to acknowledge the valuable discussions with Dr R. L. Stamps.

References

[1] S. Sun, C. B. Murray, D. Weller, L. Folks, A. Moser, "Monodisperse FePt Nanoparticles and Ferromagnetic FePt Nanocrystal Superlattices", Science, **287**, 2000, 1989.

[2] S. Sun, E F Fullerton, D Weller CB Murray, "Compositionally controlled FePt nanoparticle materials", IEEE Trans. Magn., **37**, (2001), 1239-1243

[3] N. I. Vlasova, G. S. Kandaurova, N. N. Shchegoleva, "Effect of polytwinned microstructure on the magnetic domain structure and hysteresis properties of the CoPt-type alloys", J. Magn. Magn. Mater., **222**, (2000), 138-158

[4] E. F. Kneller K Hawig, "The exchange-spring magnet: A new material principle for permanent magnets", IEEE Trans. Magn., **27**, (1991), 3588

[5] A. C. Hindmarsh, L. R. Petzold, "Algorithms and software for ordinary differential equations and differential-algebraic equations. II. Higher-order methods and software packages" Computers in Physics **9** (1995) 148.

[6] D. R. Fredkin, T. R. Koehler, "Hybrid method for computing demagnetizing fields" IEEE Trans. Magn. **26** (1990) 415.

[7] Estimated from the Curie temperature and published values of A in CoPt in "Permanent Magnetism" R. Skomski and J. M. D. Coey, IOP Publishing, Bristol 1999.

[8] E. C. Stoner and E. P. Wohlfarth, "A mechanism of magnetic hysteresis in heterogeneous alloys", *Philos. Trans. R. Soc. London, Ser. A,* **A240**, 599-642, 1948

[9] B. Bian, K. Sato, Y. Hirotsu, A. Makino, "Ordering of island-like FePt crystallites with orientations", Appl. Phys. Lett., **75**, 1999, 3686.

[10] M. Watanabe, T. Masumoto, D. H. Ping, and K. Hono, "Microstructure and magnetic properties of FePt–Al–O granular thin films" Appl. Phys. Lett., **76**, (2000), 3971-3973

[11] Y. Tanaka, N. Kimura, K. Hono, K. Yasuda and T. Sakurai, "Microstructures and magnetic properties of Fe-Pt permanent magnets", J. Magn. Magn. Mater., 170. (1997) 289-297

[12] F.T. Parker, M.W. Foster, D.T. Margulies and A.E. Berkowitz, "Spin canting, surface magnetization, and finite-size effects in γ-Fe_2O_3 particles", Phys. Rev. B, 47, (1993) 7885-7891